applied sciences

MDPI

*Review*

# Mirrors for Space Telescopes: Degradation Issues

**Denis Garoli [1,*], Luis V. Rodriguez De Marcos [2], Juan I. Larruquert [3], Alain J. Corso [4], Remo Proietti Zaccaria [5,6] and Maria G. Pelizzo [4]**

1 Faculty of Science and Technology, Free University of Bozen, Piazza Università 5, 39100 Bolzano, Italy
2 NASA Goddard Space Flight Center (CRESST II), The Catholic University of America, 620 Michigan Ave., Washington, DC 20064, USA; luis.v.rodriguezdemarcos@nasa.gov
3 GOLD—Instituto de Optica—Consejo Superior de Investigaciones Científicas, Serrano 144, 28006 Madrid, Spain; j.larruquert@csic.es
4 CNR-IFN, Via Trasea 7, 35127 Padova, Italy; alain.corso@pd.ifn.cnr.it (A.J.C.); pelizzo@dei.unipd.it (M.G.P.)
5 Istituto Italiano di Tecnologia, Via Morego 30, 16136 Genova, Italy; remo.proietti@iit.it
6 Cixi Institute of Biomedical Engineering, Ningbo Institute of Materials Technology and Engineering, Chinese Academy of Sciences, Zhongguan West Road 1219, Ningbo 315201, China
* Correspondence: denis.garoli@unibz.it

Received: 5 October 2020; Accepted: 21 October 2020; Published: 26 October 2020


**Abstract:** Mirrors are a subset of optical components essential for the success of current and future space missions. Most of the telescopes for space programs ranging from earth observation to astrophysics and covering the whole electromagnetic spectrum from x-rays to far-infrared are based on reflective optics. Mirrors operate in diverse and harsh environments that range from low-earth orbit to interplanetary orbits and deep space. The operational life of space observatories spans from minutes (sounding rockets) to decades (large observatories), and the performance of the mirrors within the mission lifetime is susceptible to degrading, resulting in a drop in the instrument throughput, which in turn affects the scientific return. Therefore, the knowledge of potential degradation mechanisms, how they affect mirror performance, and how to prevent them is of paramount importance to ensure the long-term success of space telescopes. In this review, we report an overview of current mirror technology for space missions with a focus on the importance of the degradation and radiation resistance of coating materials. Special attention is given to degradation effects on mirrors for far and extreme UV, as in these ranges the degradation is enhanced by the strong absorption of most contaminants.

**Keywords:** space optics; mirrors; coatings; radiation; thin film; multilayer; degradation; contamination; space qualification

## 1. Mirror Technology

The trend for the future space missions is the use of high-resolution, large bandwidth telescopes [1–3]. This will require new optical systems with large apertures and extreme operation conditions. Examples are mission concepts such as Large Ultraviolet Optical Infrared Surveyor (LUVOIR), HabEx, the Galaxy Evolution Probe, and x-ray observatories [4–7]. These and many other present and future space concepts [8] introduce new challenges in mirror technologies, from the optical design to the substrate and the coatings. Mirrors are critical components in space telescopes, which are extensively used for the observations of Earth and astronomical objects. Mirror technology is evolving continuously due to improvements in materials, design, manufacture, and metrology. The main advantages of mirrors with respect to refractive optics such as lenses are the following: (i) they can work over a very wide spectral bandwidth (achromat); (ii) they can be manufactured with different shapes and large dimensions compared to lenses; (iii) they are suitable for scanning devices;

(iv) for some applications such as X-ray optics, grazing incidence mirrors are the only option available. Future large telescopes will cover an increased spectral range of observation with a broad range of multi-spectral and hyper-spectral instruments, and this can be achieved only with reflective telescopes.

A mirror consists of a substrate and, most often, a coating. Substrates can be selected among a limited number of materials. The fundamental parameters are: (i) specific stiffness; (ii) thermal stability, (iii) space environmental resistance, (iv) achievable surface quality, (v) weight, and (vi) financial aspects. Regarding the choice of mirror substrates, extensive work has been performed and reported [2,9–12].

Al or Al alloys, Be, Si, SiC, Zerodur®, nickel, and fused silica have been employed [2,3,10,12,13], although glass has been the most used material for mirror substrates, given its thermal stability and ease of engineering into high-quality optical surfaces [14]; for instance, it is used as substrate in the Hubble Space Telescope, the largest space mirror still operating. However, one important shortcoming of using glass is its weight, which often limits its use to small-aperture mirrors. For this reason, new materials have been developed, with near future state-of-the-art mirror research focusing on segmented mirrors prepared on Zerodur, Be, Al, Si, or SiC substrates [14]. New large telescopes with active mirrors are now being developed with carbon-based (lightweight) materials. Silicon carbide (SiC), in particular, has been successfully used in the European Space Agency (ESA) Herschel Space Observatory [15], and it is still extensively investigated as a potential standard because of its superior stiffness, strength, and thermal properties [16,17]. Additionally, as illustrated by M. Bavdaz et al. [18], Silicon Pore Optics (SPO) is the new X-ray optics technology under development in Europe, forming the ESA baseline technology for the International X-ray Observatory candidate mission studied jointly by ESA, NASA, and Japan Aerospace Exploration Agency (JAXA).

As mirror substrates do not always provide the desired optical performance, the use of optical coatings to improve them is often required. Coatings have a major impact on the instrument optical performance. Even if mirrors are insensitive to chromatic aberrations, the need for large spectral bandwidth impacts the coating design and the technologies to reach broadband reflective coatings with a high reflectivity and low coating-induced polarization. In particular, while most mirrors used for space systems that operate from the ultraviolet (UV) to the infrared (IR) wavelength regions rely on coatings of Ag, Al, Au, or Be, extreme regions such as X-Ray, extreme UV (EUV), and far-IR require specific engineered designs comprising many layers of different materials. The coating may include adhesion layers (between the substrate and/or layers with poor adhesion), interdiffusion layers (between layers of different species) and protection or enhancement layers (on top of the reflective layer or multilayer). Dielectric optical coatings can be used alone or in combination with metallic ones in multilayers. Multilayers of metal-dielectric and all-dielectric films have been extensively used to prepare narrow band reflectors for several spectral bands [19–21]. Multilayers consist of several layers of two or more materials with optimized thicknesses to obtain the desired spectral, angular, and/or polarization profile. In the visible and close ranges, multilayers alternate layers of transparent (dielectric) materials, which enables the theoretical design of virtually any arbitrary profile. In ranges such as extreme UV and soft x-rays, where materials are characterized by high absorption, multilayers may typically alternate a dielectric material and a metal or even two metals. With the introduction of EUV lithography [22]—using 13.5 nm photons—in the semiconductor industry, the understanding and development of such multilayer structures and the overall and long-term performance of such optical systems have received a boost over the last few decades. Inside these lithographic machines, optical multilayer components are not only exposed to high fluxes of EUV radiation, but also to a peculiar type of plasma which is induced by the photo-ionization of the low-pressure background gas inside these machines [23,24]. The impact of this overall plasma+photon atmosphere on the multilayer structures used can be both disadvantages (e.g., carbon deposition [25], silicon oxidation [26], and blister formation [27,28]) and advantageous (e.g., plasma cleaning [29]).

The success or failure of a space observatory depends on the stability of each subsystem, including its optics and detectors. The extreme environment where they must operate implies severe issues in terms of stability and resistance.

## 2. Degradation of Materials in Space—Stability Issues on Mirrors

Common to all orbits is the degradation of materials by the hazardous space environment, whose importance in space technology is undeniable [30,31]. Degradation may be caused by atomic oxygen, thermal stress, electromagnetic radiation, telescope outgassing or self-contamination, charged particles, space debris, and micro-meteorites. In Low Earth Orbits (LEOs), atomic oxygen (AO) is the main source of degradation, while in the interplanetary medium the solar wind and solar electromagnetic radiation dominate the degradation effects. Most of the materials used for space optics need to be evaluated for their behavior under several of the aforementioned degradation mechanisms. It is known that these degradation mechanisms can significantly degrade materials and lead to changes in their mechanical behavior or thermo-optical properties [30]. These changes can cause early failures of satellite components or even failures of complete space missions.

The main challenge in the assessment of the degradation of materials in space is the development and choice of the most representative ground testing and extrapolation to end of-life conditions for the thermal cycle and for the charged particles, AO, UV irradiation, and high-velocity impacts of microparticles. These tests have to account for the different environments in which the mirrors will operate, ranging from Low Earth Orbit (LEO) to interplanetary orbits and deep space.

Investigations of the behavior of optical materials and coatings in the space environment started being reported in the 1970s. Pre-launch acceptance testing and the evaluation of mirrors coated for use in space are almost never performed on the actual flight mirror. Smaller witness mirrors, coated at the same time as the flight component, are used as test proxies for the spaceflight component. The intent of the acceptance testing is generally to identify any mirror surface quality problems before performing the qualification testing of the final and larger mirror. The use of test samples to verify the performances of the whole mirror is even more important for complex optical coatings such as reflective multilayers [32,33]. Environmental tests are performed to check the resistance of a mirror coating that is exposed to ambient conditions simulating the space environment for the instrument lifetime. As an example, Figure 1 shows reflectance degradation as a function of wavelength in the UV-Vis spectral range of protected Ag mirrors under various degradation sources. This combination of environmental resistance tests helps to predict, model, and account for the in-orbit degradation of the optical system.

For each of the key degradation sources (i.e., AO, UV radiation, thermal cycling, charged particles, telescope outgassing, and space debris and dust), several mitigation techniques and strategies have been proposed, most of them based on the use of protective coatings. Coatings performing critical optical functions have been used in space instrument applications for NASA, ESA and other international and national space agencies for more than 50 years. The performance of earlier coatings launched into space has been observed to change with time. Starting from that, pre-flight testing in simulated space environments has been developed to verify the spectral and efficiency performance, which are desirably able to predict the changes observed in space.

The effect of real or simulated space conditions on mirrors has been investigated during the last few decades, and in the following sections we will discuss the main results and developments reported in the literature. The next subsections address the main degradation sources in the space environment. A large emphasis is given to far UV (FUV, $\lambda$ in the 100–200 nm) and extreme UV (EUV, $\lambda$ in the 10–100 nm) due to the enhanced degradation that arises due to the strong absorption of most contaminants in these ranges compared to longer wavelengths.

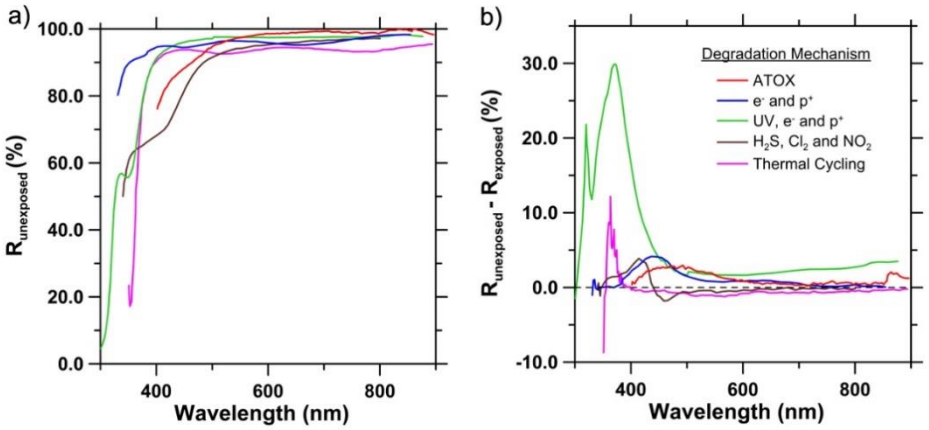


**Figure 1.** Overview of different degradation effects on a silver mirror. (**a**) Reflectivity of protected Ag mirrors from several bibliographic sources, unexposed. The differences in the mirror spectral performance are explained by the differences in the composition and thickness of the protective coatings on the Ag layer. (**b**) Effect of several degradation mechanisms on the reflectivity of protected Ag mirrors. Red curve: degradation after 37 h of exposure to a 5eV AO beam ($4 \times 10^{20}$ atom/cm$^2$) [34]. Blue curve: degradation after 279 h of simultaneous exposure to 10 keV electrons ($5.3 \times 10^{15}$ e$^-$/cm$^2$), 2 keV protons ($3.5 \times 10^{14}$ p$^+$/cm$^2$), and 5 keV protons ($3.4 \times 10^{14}$ p$^+$/cm$^2$) [35]. Green curve: degradation after 1436 h of simultaneous exposure to solar-equivalent UV, 10 keV electrons ($1.4 \times 10^{18}$ e$^-$/cm$^2$), and 5 keV protons ($1.6 \times 10^{17}$ p$^+$/cm$^2$). These dosage levels are equivalent to the radiation exposure at the L2 orbit location over a 5-year mission lifetime [36]. Brown curve: degradation after 240 h of simultaneous exposure to purified air mixed with $Cl_2$ (10 ppb), $H_2S$ (10 ppb), and $NO_2$ (200 ppb), at 30 °C and a 70% relative humidity. These conditions are fairly similar to pre-launch environments [37]. Magenta curve: degradation after 30 thermal cycles from −80 to +35 °C [38].

### *2.1. Atomic Oxygen*

AO is the main atmospheric component in LEO at altitudes of up 700 km. It is a species with large harmful potential over many materials. As a free radical of a very electronegative element, it has an intrinsic reactive capacity, which, added up to the relative velocity between the orbiting spacecraft and the thermal distribution of orbital AO, strengthens oxygen's capacity to react with and sputter off the target material. It is also an indirect source of contamination, as its interaction with organic materials, such as polymers, may originate secondary volatile compounds, which in turn might condensate on critical elements of the telescope, such as on optical surfaces. Optical surfaces are degraded in a level directly proportional to AO fluence. This, in turn, is determined by several factors, including [39] spacecraft altitude, as AO decreases with altitude; optical surfaces orientation, as surfaces in the ram or windward direction will be exposed the most; orbital inclination, as high-inclination orbits expose optics to cosmic radiation, which in turn may increase the AO generation and hence exposure; solar activity, as the Sun emits radiation and charged particles that can promote the generation of AO; and mission duration. The degradation issues caused by the impact of AO in the space environment have been investigated by several authors [40]. AO is particularly harmful in LEO, where it is formed through molecular oxygen dissociation promoted by solar UV radiation at altitudes greater than 100 km. When combined with the typical spacecraft orbital velocities of several km/sec, it has the effect of exposing the optical system to a stream of AO at an energy of approximately 5 eV. Hence, the optical components intended to operate in LEOs need to be designed to resist atomic oxygen. Nowadays, most of the flight optics undergo a critical 5 eV energy AO test for their space qualification, where the AO total fluence and exposure time on the coatings is typically calculated from numerical models and intended to mimic the extent of the entire mission [41].

While most of the oxide-based substrates are resistant to AO, bare metal surfaces and coatings may be vulnerable. The Evaluation of Oxygen Interactions with Materials III (EOIM-III) experiment tested

the resistance of several optical materials to AO during space shuttle mission 46 [42]. Among the most interesting results, coating materials such as fluorides ($MgF_2$, $CaF_2$, and LiF) and Ir and Pt showed no significant damage, but Ni mirrors showed oxide formation and the reflectivity of Au mirrors overcoated with Ni diminished because of the degradation of Ni. W. Duan et al. [43] investigated the effect of space AO on the polarization contrast of polarization-modulated mirrors under different experimental doses using a terrestrial simulator. Peters et al. [44] exposed Os, C, and bare Ag to ambient AO in a space shuttle flight. Post-flight laboratory analysis revealed that the unshielded C and Os films were totally removed, presumably by the formation of volatile oxides. Bare Ag was drastically modified to a nonconductor. Various attempts have been carried out in order to use metals as protective layers. An attempt to protect Os with a 6 nm-thick Pt film failed since the structure did not resist exposure to AO in the orbital direction and volatile Os oxide escaped through gaps in the Pt film, which resulted in poor UV reflectance measurements on both the unexposed as well as the exposed areas; on the other hand, a 10 nm-thick film of Pt provided almost complete protection [45]. However, such protection thickness would hinder the relatively large EUV reflectance of Os. Another experiment on protecting Os in order to avoid AO attack was carried out by Hemphill et al. [46]. A 2 to 3 nm-thick Ir film was seen to protect an Os film, which had been deposited either on a Rh film or on a second Ir film. Such a 3-layer structure preserved the Os' high EUV reflectance characteristic at the grazing incidences used on gratings in the 9-26 nm spectral range. Peters et al. [47] exposed films of various metals to a long LEO exposure. All materials—Cu, Ni, Pt, Au, Sn, Mo, and W—were somewhat affected by oxidation with AO, mostly in the ram direction of the spacecraft, although they were not affected as severely as had been found for Os, C, and Ag. Oxidation ranged between Au, the most stable, and Cu, the most affected. The effect of LEO AO on C was also analyzed by Hadaway et al. [48], who exposed diamond-like C (along with 12 other materials) to an LEO environment and measured the total integrated scattering in situ over time. After several weeks, the C film was completely eroded away. Gull et al. [49] exposed films of Os, Cr, Pt, and Ir to the LEO environment for a few days, and its effect on EUV reflectance was measured. Os was the most severely affected when exposed to the ram direction, in which case it was fully removed, whereas there was little change when it was masked. Cr, Pt, and Ir were much less affected. Ir underwent some reflectance decrease at wavelengths longer than 160 nm. Pt increased reflectance after exposure, which was attributed to the cleaning effect of AO on a sample that was assumed to be previously contaminated. As mentioned above, the presence of AO on the orbit may not only degrade the coating, but it also has the potential to remove contaminants from various types of coatings.

Herzig et al. [50] also exposed transition-metal mirrors of Au, Ir, Os, and Pt to a LEO environment, close to the ram direction. As with the aforementioned experiments, Os was fully removed, whereas Pt and Ir behaved relatively well after exposure. Au suffered a severe reflectance decrease, but even though some outer monolayers may have been sputtered off the decrease was attributed to contamination from the surrounding areas. The same authors also exposed chemical vapor-deposited (CVD) SiC to an LEO environment and found that its Extreme Ultraviolet (EUV)-Far Ultraviolet (FUV) reflectance was severely affected, and the degradation was much larger for the exposed area than for a masked area. Degradation was attributed to surface oxidation to $SiO_2$. The effect of AO on the CVD-SiC EUV-FUV reflectance and the synergic effect of AO along with UV radiation on the CVD-SiC near-UV reflectance were reported by G. Raikar et al. [51] and S. Mileti et al. [52], respectively. The loss in performance does not exclude the use of CVD-SiC for missions where oxygen is not present. Other than high-temperature CVD-SiC, the carbides deposited by sputtering at room temperature are a choice of moderate EUV-reflectance mirror that is attractive for optical coatings [53,54]. Keski-Kuha et al. [55] tested the ability of ion-beam-sputtered deposited SiC and $B_4C$ to withstand the exposure to the LEO AO. For SiC, a severe reflectance decrease was observed when the coating was oriented in the ram direction, and it was measured that the presence of silicon oxide on the surface was three times larger than for the witness sample kept in the lab, which was attributed to the direct exposure to AO. A second SiC sample was exposed to LEO AO, but it was placed at 160° from the ram direction, so that it was

protected from the effects related to direct AO bombardment. This sample displayed only a slight reflectance degradation, typical of an aged sample. Three $B_4C$ samples were also exposed to LEO AO at 0°, 26°, and 160° from the ram direction. All three samples experienced some EUV reflectance reduction, larger than the typical sample ageing, but the reduction was not as drastic as with SiC. The extra $B_4C$ reflectance reduction was mostly attributed to contamination. No roughness increase was observed for either SiC or $B_4C$.

Herzig et al. [50] flew Al/$MgF_2$ mirrors and exposed them to LEO environment. Even though some samples maintained their FUV reflectance, one sample experienced significant reflectance degradation at around 155 nm, and smaller degradation was observed at wavelengths of ~120 nm and 200 nm. Degradation could be attributed to contamination, since the largest sensitivity to contamination was expected to be at ~154 nm, where the intensity of the electric field on the coating surface is maximum for a 25 nm-thick $MgF_2$ protective layer. The change at 150 nm could be also attributed to the plasma resonance absorption in Al induced by surface roughness, even though no significant difference in roughness before and after orbit exposure was observed.

To reduce or eliminate the atomic oxygen erosion in materials in space, the application of thin-film protective coatings made of durable dielectric materials is the most used approach [34,35,56–60]. As previously described, oxides and fluorides are materials that are relatively resistant to AO, making them suitable as capping layers in coatings for space optics. For example, I. Gouzman et al. reported on the durability of protected silver surfaces in an AO environment [34]. In this case, the protective layer consisted of a thin $Al_2O_3$ film, as alumina has been considered one of the suitable material choices to be applied as a protective coating because of its good adhesion to Ag and passivation properties. Interestingly, they applied two approaches to test AO resistance: radio-frequency (RF) oxygen plasma exposure and a laser detonation source of 5 eV AO. It was suggested that the RF plasma environment is too severe for a realistic simulation of the AO interaction, while a 5 eV AO exposure demonstrated that the protective coating was suitable for potential LEO applications. Silicon dioxide ($SiO_2$) and magnesium fluoride ($MgF_2$) are other commonly used protective coatings in the vacuum ultraviolet (VUV) spectral region because of their high transparency down to 110 nm. $MgF_2$ coating, for example, is used as a protective layer on Al in Hubble Space Telescope optics, covering the wavelength range from 110 nm to near infrared. Even though it is quite effective, $MgF_2$-protected aluminum is a soft coating that scratches easily [3]. Therefore, optical components including a top layer of this material have to be handled carefully to avoid damage. Lithium fluoride (LiF) can extend the useful reflectance range of aluminum down to the LiF absorption cutoff of 102.5 nm. However, LiF thin films are hygroscopic and exhibit reflectance degradation and increased scattering with age.

Al high intrinsic reflectance extends beyond $MgF_2$ and LiF cutoff wavelengths down to ~83 nm. However, Al reactivity in the presence of oxygen results in a dramatic FUV/EUV reflectance decrease, and no transparent material is available in nature to preserve reflectance to such a short wavelength. Al extended reflectance was not ignored by space instrument developers since early in the space era, and such an extension would be very beneficial for space observations due to the presence of important spectral lines in the extended region. There have been several proposals to make use of Al extended reflectance in space telescopes, mostly based on aluminization in a natural ultra-high vacuum at a high enough orbit [61]. In order to implement this technology, the degradation of the FUV reflectance of unprotected Al through controlled oxidation to $O_2$, $H_2O$, and other species [62,63] and to AO [64,65] has been investigated. AO was found to be orders of magnitude more effective at degrading Al reflectance compared with the same doses of $O_2$. Non-protected Al mirrors have been also exposed to an LEO environment [50]; even though Al oxidation occurs rapidly, which happened right after the sample was taken out of the vacuum chamber in the lab, Al mirrors experienced further reflectance losses below 250 nm once in orbit, which was attributed to the greater reactivity of Al with AO compared to atmospheric $O_2$. In view of the sensitivity of bare Al reacting with AO, some procedure to significantly reduce the rate of impingement of oxidizing species must be developed, either based

on the selection of high orbits [66] or through the use of some scheme that shields the mirrors from ambient oxygen [67,68].

### 2.2. Thermal Processes

Thermal cycling may cause mechanical defects that can grow and degrade the optical system performance in orbit. For instance, strong thermal fluctuations may induce mechanical stress that may lead to alterations in the figure of the optics [69], modify the stress balance between the coating and substrate or even between different materials within the coating. Nowadays, most of the flight optics undergo a critical thermal cycling test for their space qualification. This test exposes optics to one or more cycles over temperature ranges typically within [−100 °C, +100 °C] for 24 h or more, although for some missions this test might be more extreme. As a reference, MIL-M-13508C specifies that protective Al coatings located in front mirrors have to survive at least 5h at −62 °C and 5 h at 71 °C. One example of an extreme temperature range test was the coating qualification of the oxide-protected Au-coated Be mirrors for JWST, in which witness samples were cryogenically cycled to down to 15 K four times and to 328 K one time [70].

Among others, R. K. Banyal et al. reported on thermal characteristics of a classical solar telescope primary mirror [71] (similar investigations have been reported by L. Rong et al. [72]). They used a heat transfer model that considers the heating caused by a smooth and gradual increase in the solar flux during the day-time observations and cooling resulting from the exponentially decaying ambient temperature at night. The thermal and structural response of SiC and Zerodur was investigated in detail. The low thermal conductivity of Zerodur mirror gives rise to strong radial and axial temperature gradients for daytime heating and nighttime cooling. Heat loss by free convection is very slow, so the mirror retains significant heat during the night. The observed thermal response of the SiC mirror is significantly different from Zerodur. The temperature within the SiC mirror substrate equilibrates rather quickly due to its high thermal conductivity. The thermal expansion of ceramic, silicon, and SiC optical substrate materials was also investigated in regard to Herschel (2009–2013) observatory [15]. In particular, SiC is one of the most investigated materials for an observatory in cryogenic environment [8,71,73–75].

Research on coatings and thin films demonstrated that the instability of properties in optical film was attributed both to the coating materials and their deposition process [35,38,59,76–78]. For example, with respect to metals, metal oxide compound coating materials possess large energy gaps and provide a high transmission to short, near-UV wavelengths because their optical absorption edge is outside (shorter than) the wavelength of interest. Therefore, they are intrinsically less vulnerable to damaging by thermal effect, ionizing, and UV radiation. The most commonly used coating materials are $MgF_2$, $ZrO_2$, $TaO_5$, $TiO_2$, $HfO_2$, and $SiO_2$ [79].

### 2.3. Ultraviolet Radiation

UV radiation comprises the spectral range of wavelengths between 10 nanometers up to 400 nm. The effects of high-energy photons on mirrors are not strictly related to their reflectivity or morphological properties. The effects from these photons are not the determining factor contributing to radiation damage. However, chemical changes such as reduction and oxidation reactions can induce optical absorption in thin-film layers, and UV photons can promote such reactions, changing the composition of the materials. For these reasons, space UV and ionizing radiation, the durability of materials must be considered. Importantly, the radiation effects are synergistic with other effects and must be considered together [80]. One of the principal effects of UV radiation is the polymerization and darkening of silicones and hydrocarbons, which are ubiquitous contaminants in space telescopes. This darkening effect is often enhanced by electron irradiation [81]. Hence, the UV resistance of mirrors is often tested during space qualification tests. It is common to use a distribution of Xe lamps (or similar sources) to obtain a spectral intensity profile similar to the solar irradiance, and the mirrors are exposed for a time equivalent to the intended operation hours under solar ultraviolet exposure [82].

UV exposure may have effects on polymers and other materials used in lightweight mirror material in spacecraft applications. In this latter case, the effects of UV exposure need to be accounted for due to their potential impacts on the thermal management of a spacecraft during application in composite mirror structures [83–85].

The earlier space optical thin films used for band-pass filters were based on thermally evaporated soft materials such as ZnS and $MgF_2$. Exposure to the space environment containing ionizing radiation, solar UV, atomic oxygen, and high vacuum revealed the unstable operation of those coatings. ZnS deposited by evaporation was used as a coating material decades ago for its moderate FUV reflectance and its transparency above 400 nm. Hass et al. [86] evaluated the resistance of a ZnS film to intense UV irradiation, as it would be expected in a space instrument. ZnS experienced a dramatic reflectance decrease in UV after a long UV irradiation in air, whereas the reflectance decrease was relatively small at wavelengths around 400 nm. The outermost 15–20 nm thickness was seen to have changed from polycrystalline ZnS to amorphous ZnO. The authors also studied a multilayer with single Al and Ge films under the outermost ZnS film to enhance the FUV reflectance and to decrease the near UV and visible reflectance. The Ge/Al/ZnS multilayer was UV irradiated in vacuum, which resulted in a severe FUV reflectance decrease and increasingly more severe towards shorter wavelengths, whereas no change was observed at wavelengths around 260 nm. Again, there was a predominant presence of oxygen over sulfur in the outermost 10–20 nm. The paper reported that, even in the total absence of oxygen upon UV irradiation, sulfur is expected to sublime, leaving a metallic film of Zn. All these behaviors recommend caution in employing ZnS as the outer coating of optics in space.

Fuqua at al. [87] reported the on-orbit degradation of Ag mirrors on the Suomi-NPP spacecraft. They identified an important degradation in near-IR bands of the Visible Infrared Imaging Radiometer Suite instrument, but little degradation in the green and blue channels. They first considered the possibility that the mirrors had become contaminated either before launching or on-orbit, and that the contaminant was darkening with UV exposure. However, the spectral signature of the degradation was uncharacteristic of UV darkened molecular contamination, which typically results in greater losses in the short wavelengths rather than the NIR. After an investigation on flight witness mirrors, they concluded that a non-qualified process was employed in the production of the flight mirrors, which inadvertently caused the deposition of a thin layer of tungsten oxide, WOx, on the surface of the mirrors. Tungsten oxide, when illuminated with UV, becomes absorptive in the near infrared with a spectral dependence that compared very well with the inferred behavior of the mirrors on orbit.

### *2.4. Outgassing and Cross-Contamination*

As previously mentioned, one of the main contamination sources for space mirrors originates from outgassing in the space vacuum environment, mostly from components within the telescope. Due to the strong absorption of materials, particularly contaminants in the FUV range, instrument outgassing has been investigated by several authors and the FUV properties of most volatile spacecraft materials have been measured [66,88–91], the results suggesting larger absorption in the FUV compared to longer wavelengths. These kinds of experiments are especially useful to evaluate the maximum allowable contaminant thickness before FUV reflectance is unacceptably degraded. When outgassed volatile contaminants are irradiated with strong UV radiation, this may result in the transformation of the contaminants into non-volatile compounds through a photopolymerization process, so that they may condensate/bond on the coating surface, thus degrading its optical performance. UV radiation provides the energy to break bonds in the hydrocarbon chain and stimulates intermolecular crosslinking [66]. The photopolymerization process mostly depends on the coating and contaminant nature, the substrate temperature, and the specific UV radiation energy and intensity [92]. In this respect, a facility was realized at Goddard-Space Flight Center (GSFC) to controllably contaminate mirrors and measure their FUV degradation in situ [92]. In this scenario, it is important to point out that Al, Ag, or Au-based mirrors (e.g., Al/$MgF_2$ reflectance [93]) can undergo degradation only upon the presence of contaminants

combined to UV radiation. Other than UV, energetic protons and electrons may also contribute to turn a contaminant into a non-volatile product [66].

A strong manifestation of the synergistic effects between UV and contaminants was observed after the first servicing mission on Hubble Space Telescope (HST) [94]. The Wide Field Planetary Camera I (WFPC-1) was replaced and returned to Earth where its pickoff mirror was analyzed. The Al/$MgF_2$ mirror was found to be covered with a 45 nm-thick contaminant, which severely degraded the FUV reflectance. The contamination was attributed to the outgassing of HST during its first 3.5 years of operation. The mirror was found to be contaminated with hydrocarbons, esters, and silicones. Figure 2 shows the drastic reduction in reflectivity at short wavelengths, with the x-ray photoemission spectroscopy (XPS) data revealing the composition of the contaminants. The mirror was then carefully cleaned, leading to a full restoration of the preflight reflectance, hence demonstrating no or negligible degradation of the Al/$MgF_2$ coating [94].

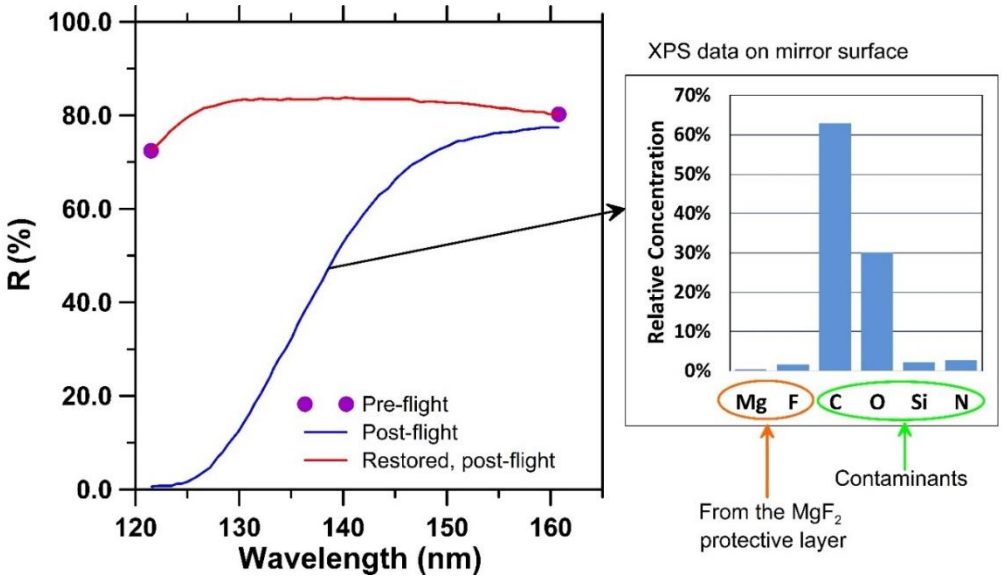


**Figure 2.** Evolution of the far-ultraviolet reflectance of the Wide Field and Planetary Camera-1 (WFPC-1) pick-off mirror (based on Al protected with $MgF_2$). Purple points: pre-flight data. Blue: post-flight data after 3.5 years of deployment in space, with a severe reflectance degradation. Red: reflectance recovery after contamination removal with a chemical cleaning. The inset on the right depicts XPS data acquired on the surface of the recovered mirror after its return to Earth, showing the presence of contaminants such as C, O, Si, and N. [95].

A later servicing mission enabled the retrieval of more Al/$MgF_2$ mirrors from the HST after 15.5 years in space [96]. While two COSTAR optics mirrors kept a relatively high FUV reflectance, comparable to or even better than a witness sample that had been stored in a desiccator, the WFPC-2 pick off mirror resulted in a reflectance degradation as severe as for the aforementioned WFPC-1 mirror. This suggested a similar contamination for both mirrors, in spite of the efforts carried out to reduce the contamination on WFPC-2 after the experience with WFPC-1. The different levels of contamination through the mirrors were unexpected and attributed to contamination dependent on the specific location within the HST hub.

Regarding grazing-incidence mirrors, Osantowski calculated the sensitivity of mirror reflectance to a range of optical constants selected for generic contaminants, such as hydrocarbons [97]. Three wavelengths were investigated as representative of the EUV: 10, 50, and 100 nm. He calculated critical contaminant thicknesses to reach allowable reflectance changes. A preliminary conclusion was that Au and Zerodur mirrors are relatively insensitive to top surface films, which can even result in an increased reflectance in some cases. Mrowka et al. investigated the effect of intentional contamination of the grazing incidence of Au mirrors with vacuum pump oil to evaluate the allowable reflectance

decrease by contaminants of an instrument part of the EUVE space telescope [98]. To check the effect of contamination with a common contaminant, a coating was contaminated with 15 nm oil. After a long-enough outgassing time in the reflectometer vacuum chamber, a total recovery of the original EUV reflectance with no increase in scattering was observed. In the case of a 50 nm-thick layer of oil, outgassing reduced such thickness just to 35 nm, and the mirrors kept a hazy look. Since the remaining oil deposit was known to be in droplet form, an increased scattering for the coating was expected. Other explanations related to polymerization were discarded because the estimates of UV irradiation and charged particle fluxes were too small to induce the observed degradation.

### 2.5. Charged Particles

An additional concern in space optics regards the mirrors degradation occurring when they are exposed to charged particles and ions. During an inter-planetary journey, galactic cosmic rays background and Sun are the main sources of such particles and ions. Galactic Cosmic Rays (GCRs) are a continuous and isotropic flow of charged particles reaching the solar system from outside the heliosphere. They are approximately composed of 85% protons, 14% helium, and the residual 1% heavy ions. The energy spectrum ranges from few MeV up to GeV with particles fluxes that decrease with increasing energy. Inside the heliosphere, GCRs decrease by a few %/Astronomic Unit (AU) with heliocentric distance (R), while the solar activity modifies the GCRs flux. As the solar activity undergoes an 11-year cycle, the GCR flux varies with the maximum during solar minimum periods [99]. The Sun emits particles such as protons, electrons, alpha particles, and less abundant heavy ions such as $O^{+6}$ and $Fe^{+10}$ continuously (solar wind), either as part of eruptions (unpredictable occurrences) or as coronal mass ejections. The solar wind is an outflow of completely ionized gas originating from the solar corona and expanding outwards to the interplanetary regions. Different components are contained in the solar wind, which differ for particle speed, the spectral flux (particles/eV $cm^2$ s) of the constituents, and the solar region of provenience. For instance, the "quiet" solar wind in the ecliptic plane is constituted by protons of ~1 keV and alpha particles of ~4 keV, whereas out of the ecliptic such energies can increase up to four times [100]. More severe but transient disturbances can be caused by energetic particles events occurring during coronal mass ejections or solar flares. These events can potentially lead to high fluxes of protons in the energy range from tens to hundreds of MeV, whose effects can be occasionally detected even on Earth surface. This proton emission occurs randomly and usually during periods of solar maxima, and it is accompanied by heavy ions. In general, the fluence of solar energetic particles scales with distance from the Sun as $R^{-3}$ at a few MeV and $R^{-2}$ at tens of MeV and above [101].

Around planets, the space environment is also affected by their magnetosphere, which interacts with charged particles present in the heliosphere. Moreover, the albedo neutrons generated by GCRs' interaction with the planet atmosphere decay into protons, giving an additional source of ions around planets. These particles are confined via magnetic mirroring and trapped preferably in some regions around the planets, forming radiation belts [102]. For example, Earth has two main electron belts at about 3000 and 25,000 km altitudes, with energies varying from few keV up to 10 MeV; protons are instead confined in a belt at around 3000 km altitudes, in which the energies span between 100 keV and several hundred MeV. Outside these radiation belts the distribution and flux of particles depends on the characteristics of the magnetosphere, the planetary atmosphere, the Sun distance and the phase of the solar cycle. Earth geostationary orbits (GEO; circular orbits at 35,786 km altitude) has an electron flux ranging between $10^9$ e/($cm^2$s) and $10^8$ e/($cm^2$s) in the energy interval 1–10 keV and $10^5$ e/($cm^2$s) at 1 MeV. The proton fluence in the same orbit is $10^{10}$ p/($cm^2$s) at 1 MeV and decreases by two orders of magnitude at 10 MeV and four at 100 MeV. The magnetosphere of giant planets, such as Jupiter, becomes an important source of high-energy electrons (>10 MeV) in interplanetary space [103].

The spacecraft components need to be protected from highly penetrating radiation and particles encountered in the operational environment. In fact, highly energetic photons as well as MeV particles can easily penetrate mm thicknesses of materials, undergoing a deceleration in the case of particles and,

in general, producing secondary photon and particle emissions. By their nature, secondary particles have to be analyzed on a case-by-case basis through Monte-Carlo simulation in order to obtain global information that can be used during the design and testing procedures. For this reason, spacecraft requirements always include a total ionizing dose (TID) specification (expressed in krad), a value that corresponds to the total energy deposited in matter by ionizing radiation per unit of mass. By definition, TID is an integral dose, and therefore it takes into account the cumulative effect due to particles of different energies. The ground validation of the spacecraft components is then usually performed by evaluating the effect given by a specific TID, deposited via acceleration facilities. Although this approach is suitable for testing the radiation hardness of an electronic component or investigating the degradation of the opto-mechanical properties of bulk materials, it becomes inappropriate for the optical coatings because the effects occurring in the thin films strongly depend on the proton energy and therefore the implantation depth of particles. High-energy particles penetrate deeper in the optical components, in the order of tens of μm or more, interacting very little with the nanometric coatings and depositing all the energy in the substrate. In contrast, keV ions implant within the coatings with a profile highly dependent on their density, potentially inducing changes of their optical, structural, and morphological properties. As a general rule, we can affirm that thin films in the nanometric scale are mostly affected by low energy particles, that implant in the coating itself, but not by MeV particles, which overcome the structure, eventually reaching the substrate. For instance, considering the typical materials employed for a mirror coating, protons at 1 keV have a penetration peak at a depth of 20–30 nm; at 16 keV, the implantation peak is at 150–200 nm; at 50 keV, it is at 300–500 nm; and at 100 keV, it is around 700–900 nm. In contrast, protons at 1 MeV already penetrate the coating for different μm. Experiments with MeV electrons and protons with typical fluences faced in the space environment (i.e., $<10^{12}$ ions/cm$^2$) have proven negligible degradation effects on optical coatings having a total thickness lower than few microns in the visible-UV [104–106], in FUV [93] and even in the EUV [107]. Visible multilayer filters irradiated with protons at 4, 18, and 30 MeV [104,106] and electrons at 50 MeV [105] showed no changes after irradiation. Canfield et al. [93] irradiated Al/$MgF_2$ mirrors with 1 MeV electrons and 5 MeV protons. No effect on the reflectance at 121.6 nm was observed. Hass and Hunter [66] reported also the effect of energetic electrons and protons on Al/$MgF_2$ coatings.

The investigation of the effects induced on optical mirrors by low-energy particles and ions are typically performed by using terrestrial facilities based on ion implanters and accelerators. However, the simulation of the space environment exposure is extremely challenging, since it is extremely challenging to approach the irradiation conditions occurring in space. For example, while the exposure in space usually lasts for several years, a ground-based experiment needs high particle flux rates in order to reach the mission life-time expected fluences in a reasonable amount of time. Moreover, during the accelerating tests can arise potential synergistic effects, not present in space, such as thermal effects related to the high flux and surface contaminations due to the contaminants present in the employed vacuum chamber [108]. Moreover, irradiation experiments are also highly influenced by practical reasons, such as the availability of a facility able to provide the desired ion species, energy, and flux.

In the case of low-energy particles, the damage amount depends on the energy, flux, and fluence. Low-energy proton irradiations (<500 keV) with fluences lower than $10^{16}$ p/cm$^2$ have been shown to determine negligible changes in the near infrared reflectance of $SiO_2$-protected Al mirrors [109,110]. A degradation dependent on the proton fluence has been instead observed in the visible and near ultraviolet ranges. For example, Hai et al. and Qiang et al. [111–113] investigated the effect of 60 keV protons on Al protected with $SiO_2$. These mirrors were measured from the near UV to the IR. Reflectance was monotonously degraded with the proton dose (see Figure 3a); with a fluence of $10^{16}$ p/cm$^2$, a reflectance drop of 5% at 700 nm and 10% at 500 nm was observed, whereas in the UV range this drop goes to over 20%.

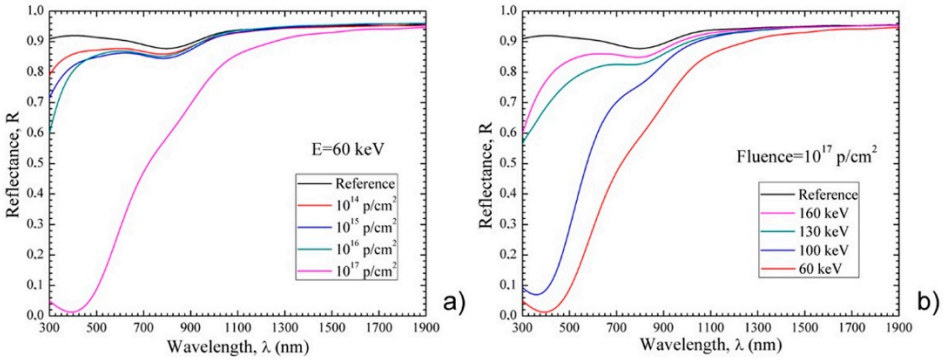


**Figure 3.** Effect of protons on mirror reflectivity. (**a**) Evolution of the UV-VIS reflectance of a $SiO_2$-protected Al mirror irradiated with protons at 60 keV with different fluences (data retrieved from [110]). (**b**) Evolution of the UV-VIS reflectance of $SiO_2$-protected Al mirror irradiated with protons at different energies and keeping a fluence of $1{\cdot}10^{17}$ p/cm$^2$ (data retrieved from [110]).

Moreover, fluences in the order of $10^{17}$ p/cm$^2$ heavily compromise the Al-protected mirror reflectance up to over 1000 nm. Similarly, Al/$MgF_2$ mirrors of unknown design but optimized for the near-UV or visible range, and hence with a thicker $MgF_2$ protective coating than FUV mirrors, were exposed to a geostationary orbit simulator consisting in simultaneous irradiation with UV, electrons and protons [80]. The UV reflectance decay was found to depend on the specific mirror, which had been prepared by a specific vendor, so that some degradation could not be discarded for the mirrors in space environment. Such degradation may not have been due to the presence of contaminants but to the shallow penetration of electrons and even more to less penetrating protons. Such a reflectance decrease was attributed to the change of Al optical constants or to the appearance of ripples and hillocks on the surface of the Al mirror. Calculations on the effect of protons over generic metallic surfaces predict the recombination of protons to form $H_2$ bubbles, in turn resulting in a significant roughness increase. Importantly, the proton energy used in the irradiation experiments greatly influences the degradation results. For example, based on the results reported in [110], it can be observed that a fluence of $10^{17}$ p/cm$^2$ induces a higher reflectance degradation when the proton energy is low. This fluence at 60 keV induces a reflectance drop of 99% at 400 nm, while at 160 keV this drop is about 20% (see Figure 3b). This degradation is due to the different ion implantation profile inside the coating: the lower is the energy, the shallower is the ion implantation peak. In case of metallic mirrors, if the implantation peak falls in the topmost part of the metallic layer or inside an eventual protective layer, the bubble formation inside the coating will provide a greater degradation.

Gillette and Kenyon [114] exposed Al/$MgF_2$ and Al/LiF FUV mirrors to 10 keV protons to simulate several-year exposure in a synchronous earth orbit. Such irradiation resulted in a broad-band reflectance decrease centered at ~210 nm (Al/$MgF_2$) and ~190 nm (Al/LiF), with the reflectance decrease growing with the proton dose. Furthermore, for the analyzed mirrors the reflectance decrease was negligible at the short-end of the high FUV reflectance range, which was explained with the presence of contaminants but not coating degradation. The contamination thickness was calculated to be 4–5 nm. Even though an undulating pattern on the coating surface was induced by irradiation, its small width did not result in observable scattering. Most of the reflectance degradation could be reverted, hence approaching the original reflectance after exposing both Al/$MgF_2$ and Al/LiF mirrors to AO, a result attributed to the oxidation of the contaminants, which took a volatile form. Gillette and Kenyon [114] also exposed Pt mirrors to 10 keV protons to simulate a long exposure in a synchronous earth orbit. The reflectance degradation in the full 93–250 nm range presented no spectral structure, which may be due to the lack of interference, contrary to what was observed for Al/$MgF_2$ and Al/LiF mirrors.

A similar behavior was observed with He ions. Low-energy He ion irradiations on metallic thin films of Au and Cu demonstrate that, with fluences in the order of $10^{15}$–$10^{16}$ ion/cm$^2$, a faint dislocation band starts forming, with the preservation of the optical performance in the visible spectral range and a

fluence-proportional degradation in the ultraviolet range [115]. Fluences in the order of $10^{17}$ ions/cm$^2$ were found to induce a large formation of bubbles inside the films and a deep transformation of the surface morphology [116,117], with a consequent degradation of the visible and UV reflectance. The diameter and the density of such bubbles increase with the fluence due to the tendency of helium ions to migrate and form agglomerates. This behavior has been confirmed not only in metals, but also in semiconductors [118].

A particular case is instead that of multilayer (ML) stacks for the EUV. Several studies have demonstrated that protons and alpha particles with energy of a few keV can already lead to dramatic degradations of performance with fluences in the order of $10^{16}$ ions/cm$^2$ [119–121]. For example, Mo/Si structures with different capping layers were irradiated by protons at 1 keV with fluences of $9{\cdot}10^{15}$ and $36{\cdot}10^{15}$ p/cm$^2$, showing a change in the peak position and a degradation of the reflectance (Figure 4a). Such an effect was attributed to the expansion and delamination occurring in the topmost layers of the ML stack (see the TEM image reported in Figure 4b) [122–124]. After the $He^+$ ion irradiation with fluences of $2.5{\cdot}10^{15}$, $5{\cdot}10^{15}$, and $10^{16}$ ions/cm$^2$, the exposed MLs showed a drop of reflectance but no appreciable reflectance peak shifts [120]. In this case, the degradation was attributed to an increase in the intermixing at the interfaces in the topmost layers.

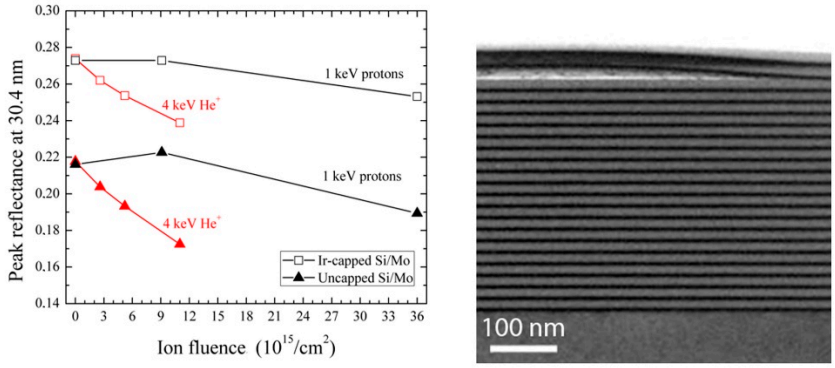


(**a**) (**b**)

**Figure 4.** Effect of charged particles on multilayer coating (**a**) Evolution of the EUV reflectance at 30.4 nm of an uncapped and Ir-capped Si/Mo multilayer coating versus 1 keV proton and 4 keV He ion fluence (data from ref. [119,120]). (**b**) Delamination occurring on a Si/Mo multilayer under a 1 keV proton irradiation with a fluence of $3.6{\cdot}10^{16}$ p/cm$^2$ (image from Ref. [119]—2011 OSA).

Recently, Al/Mo/$B_4$C and Al/Mo/SiC were also irradiated with 1 and 100 keV protons with doses of $7.4{\cdot}10^{12}$ and $9{\cdot}10^{15}$ p/cm$^2$. The lowest dose was chosen in order to simulate the situation expected inside the High Resolution Imager (HRI) and Full Sun Imager (FSI) telescopes on board of the ESA Solar Orbiter mission, where the mechanical structure and the front filters drastically reduce the proton flux impinging on the multilayers. None of the irradiated structures showed appreciable changes in performance, suggesting that at these values of fluence MLs can be considered stable.

### *2.6. Dust and Space Debris*

Dust (or meteoroids) and space debris are important sources of mirror degradation. In extreme conditions, meteoroids may cause a full spacecraft failure. One example was the Olympus communications spacecraft (ESA), in which the general failure of the satellite was attributed, with a high probability, to a Perseid meteoroid impact [125]. Although dust and debris are small in weight and size (e.g., millimeter- and micron-size particles are the most abundant in LEO), their high velocities, ranging from few m/s up to dozens of km/s, represent a threat for space optics. In the near-Earth area, space debris is generated by launch activity and subsequent operational practices, with size range between 10 μm and 1 mm [126]. However, meteoroids are generally more harmful than space debris, as the average velocity of the former is higher. Beyond LEO, space dust is dominant, where short-period

comets with aphelia less than 7 AU have been identified as a major source of interplanetary dust released through the sublimation of cometary ices [127]. Aside from the mass and velocity, the effect of these particles can be further exacerbated by the directionality of the optical surfaces relative to the ram direction. The exposure time is also critical; it has been reported that even after a short exposure to the space environment, exposed surfaces can be covered with impacts from small-size debris and meteoroids [128]. The chemical composition of dust is diverse, but most compounds are silicates, ice, iron, and organic compounds. Depending on several factors, dust can accumulate on the surface of the optics and increase the scattered radiation [129], or flake the protective coating, leaving reactive materials exposed (which could be subsequently degraded by AO, for instance), or can even blast away the coating and produce craters on the substrate. In extreme conditions, high-velocity collisions may produce plasma, generating side-effects that may be more damaging than purely mechanical effects [125]. Additionally, the collateral effects of impacts may induce the damage or contamination of the optics; an example will be provided below in the description of one of the NASA Long Duration Exposure Facility (LDEF) experiments.

Experimental verification is often necessary to better understand the effect of high-velocity particles. This can be performed in dedicated testing facilities, such as the Heidelberg Dust Accelerator, in which particles of various materials can be accelerated to velocities up to 40 km/s [130]. Heaney et al. [131] utilized the aforementioned facility to simulate the effect of the impacts of iron (1.2 μm diameter) and latex (0.75 μm diameter), o mimic inorganic- and organic-based meteoroids at velocities of 2–20 km/s on an oxide-protected, Au-coated Be witness mirrors for the James Webb Space Telescope (JWST). It was found that both latex and iron particles had the ability to blast away the protective coating, creating craters where be substrate was exposed. The authors reported ratios between the crater diameter and the incident particle kinetic energy of 0.09 μm/nJ for latex and 0.07 μm/nJ for iron. Yet, most of the knowledge of the mass and velocity distribution of the dust, composition, flux, and effect of impacts in space instrumentation has been gathered in the last decades from dedicated experiments in space, such as dust detectors on board of GALILEO and ULYSSES, or the cosmic dust analyzer (CDA) on board of CASSINI [130]. The CDA instrument had two sensors; the first one was a high-rate detector to count the number of particles, and the second one analyzed the dust's charge, speed, size, and direction. Further knowledge related to the dust and debris characteristics has been obtained from satellites or parts thereof returned from space (Shuttle, Solar Max, Palapa, Westar, MIR, EURECA, HST). As an example, the chemical analysis of the craters on solar cells recovered from the HST showed that caters with diameters of 100–3500 μm were produced by meteoroids, whereas craters with diameters of 1–100 μm were produced mostly by space debris composed of aluminum and aluminum oxide, indicative of solid rocket motor fuel debris [132]. The Long Duration Exposure Facility (LDEF) experiment deserves special mention; in this experiment, a tray with several optics was mounted in the exterior of the spacecraft (see Figure 5a,b), and exposed for 5 years and 8 months (32,422 orbits in LEO, from 842 km to 340 km) to micrometeoroids and space debris. This extended duration presented a unique opportunity to study the long-term effects of space exposure on the coatings and substrate materials flown. Among the most spectacular results, a 1 mm-diameter impact in a bare $CaF_2$ substrate produced a two-direction full cleavage, breaking the sample into three pieces, as shown in Figure 5c. Another impact on a PbTe/ZnS multilayer-coated Ge substrate caused a coating delamination in the surroundings of the spallation area of 4.5 mm diameter. Posterior analysis of the multilayer coating showed that the impact did not add stress or induce any further coating damage beyond the spallation area. The contamination of the SiO-coated Si substrate by aluminum provided the best example in the LDEF of the secondary ejecta and collateral effects of impacts. An impact occurred in the edge of the aluminum sample holder (see Figure 5d), leaving secondary ejecta spray patterns of molten aluminum on the surface of the sample [133,134].

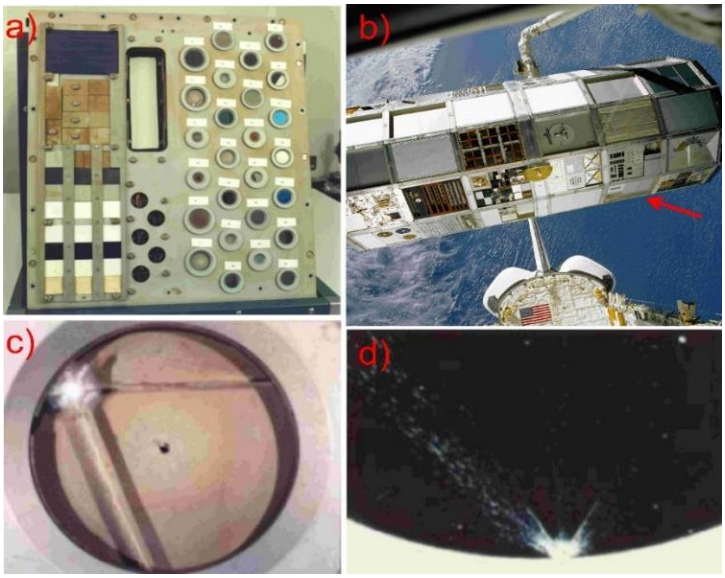


**Figure 5.** Effect of space debris (**a**) Tray B08 with several mounted optics. There were bare substrates and coated substrates, among other samples. (**b**) The LDEF in orbit. The location of tray B08 in LDEF can barely be seen, but it is indicated with a red arrow. (**c**) Impact and cleavage of the $BaF_2$ substrate. (**d**) Impact on the edge of the Al holder for the SiO-coated Si sample. Molten Al spray patterns can be seen on the sample surface (**a**,**c**,**d**) and are available at www.reading.ac.uk and https://www2.physics.ox.ac.uk, Infrared Laboratory, LDEF. (**b**) Available at the NASA Image and Video Library.

To summarize, space dust and debris can affect the performance of mirrors and coatings, or even determine a full mission failure. However, the body of spacecrafts should be protected from micrometeoroids and space debris impacts. F. Whipple proposed in 1947 [135] that a steel "skin" of one millimeter thickness spaced one inch from the main spacecraft body would disintegrate along with the high-velocity meteoroid upon impact, thus preventing the latter causing damage to the spacecraft. Even though this protective system has been verified, implemented, and improved since then, this cannot be used to protect the primary mirror of an optical telescope, for instance. Hence, the protection of exposed optical elements mostly relies on prevention and prediction. In this respect, all space agencies pursue the common goal of reducing the generation of space debris from in orbit explosions and collisions and from rockets' upper stages, and discouraging anti-satellite missile tests. In terms of prediction, models which can precisely account for (1) meteoroid velocity and mass distributions as a function of orbit altitude, (2) the flux of meteoroids of larger sizes (>100 microns), (3) the effects of plasma during impacts, and (4) variations in the meteoroid bulk density with impact velocity have been identified as a powerful tool to foresee the effect of dust and debris in future space observatories [126].

## 3. Conclusions

Optical coated elements for space instrumentation are mainly optimized in terms of their efficiency and required working spectral band. After fabrication, witness samples undergo a series of laboratory tests required by space agencies in order to qualify the components. However, laboratory tests rarely reproduce the conditions in space; because the quality of the vacuum is not the same as in space, some contaminants coming from the satellite itself are neglected. The space environment is not always known precisely, and the flux of particles and contaminants is lower in space than in accelerated tests.

Mirror substrates and coatings are the key components of space optics. Space mirrors must withstand a harsh environment, where servicing campaigns to clean or replace degraded optics are very limited or, most often, impossible. Mirrors must be able to keep acceptable performance through

missions that may have a lifetime as long as decades. In fact, the optical performance of the components strongly affects the scientific data outcomes, and their degradation can lead to data misinterpretation due to an unknown change in the instrument radiometric response. In a more dramatic scenario, unpredicted mirror degradation may kill an expensive mission along with the high expectations of the community for decades.

Hence, space opticians need to predict the behavior of coatings and substrates at the specific orbit and space conditions and for the full mission lifetime. In order to accomplish this objective, more experimental data need to be collected and shared. This is particularly important, as presently very few experimental data are made available by the re-testing of components in those few cases in which the optics have been collected after a flight. The results of qualification tests are rarely published and made available to the scientific community, as they are perceived as small technical details and because there is not a reference scientific journal which offers a solid background in this field, as is the opposite of the case of electronics components. The clear definition of testing procedures to assess the robustness of optical components against the operational environment is of pivotal importance for preventing in-flight failures, to fabricate robust coatings, or simply to model their degradation. In situ testing experiments in which simple optical systems are coupled to mirror optics for efficiency measurements over time during a flight could be an advantage.

This paper is intended to contribute to the formation of a background knowledge in the field. Attention has been devoted to the main sources of mirror degradation: atomic oxygen, thermal processes, ultraviolet radiation, outgassing and cross-contamination, charged particles, and space debris and dust. An effort has been made to cite and comment the main literature on the degradation effects of all these sources on mirrors all over the electromagnetic spectrum, with an emphasis at short wavelengths. Available information combines space simulation in the lab and also the heritage of six decades of space optics. Despite the large amount of literature on space mirrors and degradation/stability issues, significant improvements are still desired for future space observatories. The development of large size and broadband mirrors will come together with new materials and coating designs. Future low-orbit to deep-space exploration will need to keep solving new issues on the degradation resistance of mirrors.

**Author Contributions:** All the authors have contributed to prepare the manuscript. All authors have read and agreed to the published version of the manuscript.

**Funding:** JIL acknowledges funding by Ministerio de Ciencia e Innovación, Gobierno de España (PID2019-105156GB-I00). LRM appreciates the support from the Center for Research and Exploration in Space Science and Technology II (CRESST II) program. MGP acknowledges ASI-INAF I/013/12/0 Solar Orbiter, METIS instrument European Space Agency (contract no. 4000122836/18/NL/PS/gp), Radiation Testing of Optical Coatings for Space.

**Conflicts of Interest:** The authors declare no conflict of interest.

## References

1. Postman, M. Advanced Technology Large-Aperture Space Telescope: Science drivers and technology developments. *Opt. Eng.* **2012**, *51*, 011007. [CrossRef]
2. Trumper, I.; Hallibert, P.; Arenberg, J.W.; Kunieda, H.; Guyon, O.; Stahl, H.P.; Kim, D.W. Optics technology for large-aperture space telescopes: From fabrication to final acceptance tests. *Adv. Opt. Photonics* **2018**, *10*, 644. [CrossRef]
3. Feinberg, L. Space telescope design considerations. *Opt. Eng.* **2012**, *51*, 011006. [CrossRef]
4. Gaier, T.; Mikhail, R.; Cavaco, J.; Vayda, J.; Steeves, J.; Wallace, J.K.; Redding, D.; Lawrence, C.; Bartman, R. Active mirrors for future space telescopes. In *Advances in Optical and Mechanical Technologies for Telescopes and Instrumentation III, Proceedings of the SPIE Astronomical Telescopes + Instrumentation, Austin, TX, USA, 10–15 June 2018*; Geyl, R., Navarro, R., Eds.; SPIE: Bellingham, WA, USA, 2018; 38p.
5. Bolcar, M.R.; Balasubramanian, K.; Clampin, M.; Crooke, J.; Feinberg, L.; Postman, M.; Quijada, M.; Rauscher, B.; Redding, D.; Rioux, N.; et al. Technology development for the Advanced Technology Large Aperture Space Telescope (ATLAST) as a candidate large UV-Optical-Infrared (LUVOIR) surveyor. In *UV/Optical/IR Space Telescopes and Instruments: Innovative Technologies and Concepts VII, Proceedings of the*

*SPIE Conference Proceeding, San Diego, CA, USA, 9–13 August 2015*; MacEwen, H.A., Breckinridge, J.B., Eds.; SPIE: Bellingham, WA, USA, 2015; p. 960209.

6. Bolcar, M.R.; Balasubramanian, K.; Crooke, J.; Feinberg, L.; Quijada, M.; Rauscher, B.J.; Redding, D.; Rioux, N.; Shaklan, S.; Stahl, H.P.; et al. Technology gap assessment for a future large-aperture ultraviolet-optical-infrared space telescope. *J. Astron. Telesc. Instrum. Syst.* **2016**, *2*, 041209. [CrossRef] [PubMed]
7. Philip Stahl, H. Advanced ultraviolet, optical, and infrared mirror technology development for very large space telescopes. *J. Astron. Telesc. Instrum. Syst.* **2020**, *6*, 1. [CrossRef]
8. Villalba, V.; Kuiper, H.; Gill, E. Review on thermal and mechanical challenges in the development of deployable space optics. *J. Astron. Telesc. Instrum. Syst.* **2020**, *6*, 1. [CrossRef]
9. Stahl, H.P. Mirror technology roadmap for optical/IR/FIR space telescopes. In *Space Telescopes and Instrumentation I: Optical, Infrared, and Millimeter, Proceedings of the SPIE Astronomical Telescopes + Instrumentation, Orlando, FL, USA, 24–31 May 2006*; Mather, J.C., MacEwen, H.A., De Graauw, M.W.M., Eds.; SPIE: Bellingham, WA, USA, 2006; p. 626504.
10. Lewis, W.C. Space Telescope Mirror Substrate. In *Space Optics II, Proc. SPIE 0183, Space Optics II, (27 September 1979)*; International Society for Optics and Photonics: Bellingham, WA, USA, 1979; pp. 114–119.
11. Zhang, W.W.; Chan, K.-W.; Content, D.A.; Lehan, J.P.; Petre, R.; Saha, T.T.; Gubarev, M.; Jones, W.D.; O'Dell, S.L. Development of lightweight X-ray mirrors for the Constellation-X mission. In *Space Telescopes and Instrumentation II: Ultraviolet to Gamma Ray, Proceedings of the SPIE Astronomical Telescopes + Instrumentation, Orlando, FL, USA, 24–31 May 2006*; Turner, M.J.L., Hasinger, G., Eds.; SPIE: Bellingham, WA, USA, 2006; p. 62661V.
12. Parsonage, T.B. JWST beryllium telescope: Material and substrate fabrication. In *Optical Fabrication, Metrology, and Material Advancements for Telescopes, Proceedings of the SPIE Astronomical Telescopes + Instrumentation, Glasgow, UK, 21–25 June 2004*; Atad-Ettedgui, E., Dierickx, P., Eds.; SPIE: Bellingham, WA, USA, 2004; 39p.
13. Witkin, D.B.; Palusinski, I.A. Material testing of silicon carbide mirrors. In *Optical Materials and Structures Technologies IV, Proceedings of the SPIE Optical Engineering + Applications, San Diego, CA, USA, 2–6 August 2009*; Robichaud, J.L., Goodman, W.A., Eds.; SPIE: Bellingham, WA, USA, 2009; p. 742509.
14. Baiocchi, D.; Stahl, H.P. Enabling Future Space Telescopes: Mirror Technology Review and Development Roadmap. In *Astro2010—The Astronomy and Astrophysics Decadal Survey*; The National Academies of Sciences, Engineering, and Medicine: Washington, DC, USA, 2009; Volume 2010, 23p.
15. Pilbratt, G.L.; Riedinger, J.R.; Passvogel, T.; Crone, G.; Doyle, D.; Gageur, U.; Heras, A.M.; Jewell, C.; Metcalfe, L.; Ott, S.; et al. Herschel Space Observatory. *Astron. Astrophys.* **2010**, *518*, L1. [CrossRef]
16. Korhonen, T.; Keinanen, P.; Pasanen, M.; Sillanpaa, A. Polishing and testing of the 3.5 m SiC M1 mirror of the Herschel space observatory of ESA. In *Optical Fabrication, Testing, and Metrology III, Proceedings of the Optical Systems Design, Glasgow, UK, 2–5 September 2008*; Duparré, A., Geyl, R., Eds.; SPIE: Bellingham, WA, USA, 2008; p. 710218.
17. Steeves, J.; Laslandes, M.; Pellegrino, S.; Redding, D.; Bradford, S.C.; Wallace, J.K.; Barbee, T. Design, fabrication and testing of active carbon shell mirrors for space telescope applications. In *Advances in Optical and Mechanical Technologies for Telescopes and Instrumentation, Proceedings of the SPIE Astronomical Telescopes + Instrumentation, Montréal, QC, CA, 22–27 June 2014*; Navarro, R., Cunningham, C.R., Barto, A.A., Eds.; SPIE: Bellingham, WA, USA, 2014; p. 915105.
18. Bavdaz, M.; Collon, M.; Beijersbergen, M.; Wallace, K.; Wille, E. X-ray pore optics technologies and their application in space telescopes. *X-Ray Opt. Instrum.* **2010**, *2010*, 1–15. [CrossRef]
19. Piegari, A.; Bulir, J.; Krasilnikova Sytchkova, A. Variable narrow-band transmission filters for spectrometry from space 2 Fabrication process. *Appl. Opt.* **2008**, *47*, C151. [CrossRef]
20. Rodríguez-de Marcos, L.; Aznárez, J.A.; Méndez, J.A.; Larruquert, J.I.; Vidal-Dasilva, M.; Malvezzi, A.M.; Giglia, A.; Capobianco, G.; Massone, G.; Fineschi, S.; et al. Advances in far-ultraviolet reflective and transmissive coatings for space applications. In *Advances in Optical and Mechanical Technologies for Telescopes and Instrumentation II, Proceedings of the SPIE Astronomical Telescopes + Instrumentation, Edinburgh, UK, 26 June–1 July 2016*; Navarro, R., Burge, J.H., Eds.; SPIE: Bellingham, WA, USA, 2016; p. 99122E.
21. Zuccon, S.; Garoli, D.; Pelizzo, M.G.; Nicolosi, P.; Fineschi, S.; Windt, D. Multilayer coatings for multiband spectral observations. In *International Conference on Space Optics—ICSO 2006, Proceedings of the International Conference on Space Optics 2006, Noordwijk, The Netherlands, 27–30 June 2006*; Armandillo, E., Costeraste, J., Karafolas, N., Eds.; SPIE: Bellingham, WA, USA, 2017.

22. Benschop, J.; Banine, V.; Lok, S.; Loopstra, E. Extreme ultraviolet lithography: Status and prospects. *J. Vac. Sci. Technol. B* **2008**, *26*, 2204–2207. [CrossRef]
23. Van der Velden, M.H.L.; Brok, W.J.M.; Van der Mullen, J.J.A.M.; Banine, V. Kinetic simulation of an extreme ultraviolet radiation driven plasma near a multilayer mirror. *J. Appl. Phys.* **2006**, *100*, 73303. [CrossRef]
24. Beckers, J.; Van de Ven, T.; Van der Horst, R.; Astakhov, D.; Banine, V. EUV-Induced Plasma: A Peculiar Phenomenon of a Modern Lithographic Technology. *Appl. Sci.* **2019**, *9*, 2827. [CrossRef]
25. Dolgov, A.; Lopaev, D.; Lee, C.J.; Zoethout, E.; Medvedev, V.; Yakushev, O.; Bijkerk, F. Characterization of carbon contamination under ion and hot atom bombardment in a tin-plasma extreme ultraviolet light source. *Appl. Surf. Sci.* **2015**, *353*, 708–713. [CrossRef]
26. Koster, N.; Mertens, B.; Jansen, R.; Van De Runstraat, A.; Stietz, F.; Wedowski, M.; Meiling, H.; Klein, R.; Gottwald, A.; Scholze, F.; et al. Molecular contamination mitigation in EUVL by environmental control. *Microelectron. Eng.* **2002**, *61*, 65–76. [CrossRef]
27. Van den Bos, R.A.J.M.; Lee, C.J.; Benschop, J.P.H.; Bijkerk, F. Blister formation in Mo/Si multilayered structures induced by hydrogen ions. *J. Phys. D. Appl. Phys.* **2017**, *50*, 265302. [CrossRef]
28. Van den Bos, R.A.J.M.; Reshetniak, V.; Lee, C.J.; Benschop, J.; Bijkerk, F. A model for pressurized hydrogen induced thin film blisters. *J. Appl. Phys.* **2016**, *120*, 235304. [CrossRef]
29. Dolgov, A.; Lopaev, D.; Rachimova, T.; Kovalev, A.; Vasil'Eva, A.; Lee, C.J.; Krivtsun, V.M.; Yakushev, O.; Bijkerk, F. Comparison of H2 and He carbon cleaning mechanisms in extreme ultraviolet induced and surface wave discharge plasmas. *J. Phys. D Appl. Phys.* **2014**, *47*, 65205. [CrossRef]
30. De Groh, K.K.; Banks, B.A.; Miller, S.K.R.; Dever, J.A. Degradation of Spacecraft Materials. In *Handbook of Environmental Degradation of Materials*; Elsevier: Amsterdam, The Netherlands, 2018; pp. 601–645.
31. Lu, Y.; Shao, Q.; Yue, H.; Yang, F. A Review of the Space Environment Effects on Spacecraft in Different Orbits. *IEEE Access* **2019**, *7*, 93473–93488. [CrossRef]
32. Tagliaferri, G.; Basso, S.; Borghi, G.; Burkert, W.; Citterio, O.; Civitani, M.; Conconi, P.; Cotroneo, V.; Freyberg, M.; Garoli, D.; et al. Simbol-X Hard X-ray Focusing Mirrors: Results Obtained During the Phase A Study. *AIP Conf. Proc.* **2009**, *1126*, 35–40.
33. Garoli, D.; Boscolo Marchi, E.; Mattarello, V.; Bertoli, J.; Salmaso, G.; Kools, J.; Spiga, D.; Tagliaferri, G.; Pareschi, G. Enabling deposition of hard x-ray reflective coatings as an industrial manufacturing process. In *EUV and X-Ray Optics: Synergy between Laboratory and Space, Proceedings of the SPIE Optics + Optoelectronics, Prague, Czech Republic, 20–23 April 2009*; Hudec, R., Pina, L., Eds.; SPIE: Bellingham, WA, USA, 2009; p. 73600U.
34. Gouzman, I.; Grossman, E.; Murat, M.; Noter, Y.; Saar, N.; Zilberman, G.; Minton, T.K.; Garton, D.J.; Buczala, D.; Brunsvold, A. A study of atomic oxygen interactions with protected silver surfaces. *Eur. Sp. Agency Spec. Publ. ESA SP* **2003**, *2003*, 487–492.
35. Sheikh, D.A. Improved silver mirror coating for ground and space-based astronomy. In *Advances in Optical and Mechanical Technologies for Telescopes and Instrumentation II, Proceedings of the SPIE Astronomical Telescopes + Instrumentation, Edinburgh, UK, 26 June–1 July 2016*; Navarro, R., Burge, J.H., Eds.; SPIE: Bellingham, WA, USA, 2016; Volume 9912, p. 991239.
36. Heaney, J.B.; Kauder, L.R.; Freese, S.C.; Quijada, M.A. Preferred mirror coatings for UV, visible, and IR space optical instruments. In *Earth Observing Systems XVII, Proceedings of the SPIE Optical Engineering + Applications, San Diego, CA, USA, 12–16 August 2012*; Butler, J.J., Xiong, X., Gu, X., Eds.; SPIE: Bellingham, WA, USA, 2012; p. 85100F.
37. Folgner, K.A. Towards Understanding the Environmental Durability and Corrosion Behavior of Protected Silver Mirrors. Ph.D. Thesis, University of California, Los Angeles, CA, USA, 2019.
38. Sheikh, D.A.; Connell, S.J.; Dummer, R.S. Durable silver coating for Kepler Space Telescope primary mirror. Space Telescopes and Instrumentation 2008: Optical, Infrared, and Millimeter. In Proceedings of the SPIE Astronomical Telescopes + Instrumentation, Marseille, France, 23–28 June 2008; p. 70104E.
39. Dooling, D.; Finckenor, M.M. *Material Selection Guidelines to Limit Atomic Oxygen Effects on Spacecraft Surfaces*; Marshall Space Flight Center: Huntsville, AL, USA, 1999.
40. Banks, B.; Miller, S.; De Groh, K. Low Earth Orbital Atomic Oxygen Interactions with Materials. In *Proceedings of the 2nd International Energy Conversion Engineering Conference, Providence, RI, USA, 16–19 August 2004*; American Institute of Aeronautics and Astronautics: Reston, VA, USA, 2004.

41. Banks, B.A.; Stueber, T.J.; Norris, M.J. Monte Carlo Computational Modeling of the Energy Dependence of Atomic Oxygen Undercutting of Protected Polymers. In *Protection of Space Materials from the Space Environment. Space Technology Proceedings*; Springer: Berlin, Germany, 2001; pp. 1–14.
42. Koontz, S.L.; Leger, L.J.; Rickman, S.L.; Cross, J.B.; Hakes, C.L.; Bui, D.T. *Evaluation of Oxygen Interactions with Materials III—Mission and Induced Environments*; Los Alamos National Lab.: Los Alamos, NM, USA, 1994.
43. Duan, W.; Liu, B.; Li, D.; Yu, D.; Liu, D. Study on the Polarization Contrast of Polarization Modulated Mirror Affected by Simulated Space Atomic Oxygen. In *Proceedings of the Optical Interference Coatings Conference (OIC), Santa Ana Pueblo, NM, USA, 2–7 June 2019*; OSA: Washington, DC, USA, 2019.
44. Peters, P.N.; Linton, R.C.; Miller, E.R. Results of apparent atomic oxygen reactions on Ag, C, and Os exposed during the Shuttle STS-4 orbits. *Geophys. Res. Lett.* **1983**, *10*, 569–571. [CrossRef]
45. Peters, P.N.; Gregory, J.C.; Swann, J.T. Effects on optical systems from interactions with oxygen atoms in low earth orbits. *Appl. Opt.* **1986**, *25*, 1290. [CrossRef] [PubMed]
46. Hemphill, R.; Hurwitz, M.; Pelizzo, M.G. Osmium atomic-oxygen protection by an iridium overcoat for increased extreme-ultraviolet grating efficiency. *Appl. Opt.* **2003**, *42*, 5149. [CrossRef] [PubMed]
47. Peters, P.N.; Zwiener, J.M.; Gregory, J.C.; Raikar, G.N.; Christl, L.C.; Wilkes, D.R. Changes in chemical and optical properties of thin film metal mirrors on LDEF. In *Third Post-Retrieval Symposium, Proceedings of the LDEF: 69 Months in Space, Washington, DC, USA, 8–12 November 1993*; NASA Langley Research Center: Hampton, VA, USA, 1995; pp. 703–725.
48. Hadaway, J.B.; Ahmad, A.; Pezzaniti, J.L.; Chipman, R.A.; Wilkes, D.R.; Hummer, L.L.; Crandall, D.G.; Bennett, J.M. Real-time total integrated scattering measurements on the Mir spacecraft to evaluate sample degradation in space. *Appl. Opt.* **2001**, *40*, 2755. [CrossRef] [PubMed]
49. Gull, T.R.; Herzig, H.; Osantowski, J.F.; Toft, A.R. Low earth orbit environmental effects on osmium and related optical thin-film coatings. *Appl. Opt.* **1985**, *24*, 2660. [CrossRef]
50. Herzig, H.; Toft, A.R.; Fleetwood, C.M. Long-duration orbital effects on optical coating materials. *Appl. Opt.* **1993**, *32*, 1798. [CrossRef]
51. Raikar, G.N.; Gregory, J.C.; Partlow, W.D.; Herzig, H.; Choyke, W.J. Surface characterization of SiC mirrors exposed to fast atomic oxygen. *Surf. Interface Anal.* **1995**, *23*, 77–82. [CrossRef]
52. Mileti, S.; Coluzzi, P.; Marchetti, M. Degradation of silicon carbide reflective surfaces in the LEO environment. *AIP Conf. Proc.* **2009**, *1087*, 67–74.
53. Garoli, D.; Monaco, G.; Frassetto, F.; Pelizzo, M.G.; Nicolosi, P.; Armelao, L.; Mattarello, V.; Rigato, V. Thin film and multilayer coating development for the extreme ultraviolet spectral region. *Radiat. Phys. Chem.* **2006**, *75*, 1966–1971. [CrossRef]
54. Garoli, D.; Frassetto, F.; Monaco, G.; Nicolosi, P.; Pelizzo, M.-G.; Rigato, F.; Rigato, V.; Giglia, A.; Nannarone, S. Reflectance measurements and optical constants in the extreme ultraviolet-vacuum ultraviolet regions for SiC with a different C/Si ratio. *Appl. Opt.* **2006**, *45*, 5642–5650. [CrossRef]
55. Keski-Kuha, R.A.M.; Blumenstock, G.M.; Fleetwood, C.M.; Schmitt, D.-R. Effects of space exposure on ion-beam-deposited silicon-carbide and boron-carbide coatings. *Appl. Opt.* **1998**, *37*, 8038. [CrossRef] [PubMed]
56. Packirisamy, S.; Schwam, D.; Litt, M.H. Atomic oxygen resistant coatings for low earth orbit space structures. *J. Mater. Sci.* **1995**, *30*, 308–320. [CrossRef]
57. Wang, X.; Li, Y.; Qian, Y.; Qi, H.; Li, J.; Sun, J. Mechanically Robust Atomic Oxygen-Resistant Coatings Capable of Autonomously Healing Damage in Low Earth Orbit Space Environment. *Adv. Mater.* **2018**, *30*, 1803854. [CrossRef]
58. Delfini, A.; Vricella, A.; Morles, R.B.; Pastore, R.; Micheli, D.; Gugliermetti, F.; Marchetti, M. CVD nano-coating of carbon composites for space materials atomic oxygen shielding. *Procedia Struct. Integr.* **2017**, *3*, 208–216. [CrossRef]
59. Bouquet, F.L.; Helms, R.G.; Maag, C.R. Recent advances in long-lived mirrors for terrestrial and space applications. *Sol. Energy Mater.* **1987**, *16*, 423–433. [CrossRef]
60. Yoo, Y.J.; Kim, Y.J.; Kim, S.-Y.; Lee, J.H.; Kim, K.; Ko, J.H.; Lee, J.W.; Lee, B.H.; Song, Y.M. Mechanically robust antireflective moth-eye structures with a tailored coating of dielectric materials. *Opt. Mat. Express* **2019**, *9*, 4178–4186. [CrossRef]
61. Burton, W.M. Removable volatile protective coatings for aluminised mirrors used in far-ultraviolet space astronomy. *J. Phys. D Appl. Phys.* **1983**, *16*, L129–L132. [CrossRef]

62. Edmends, J.; Maldé, C.; Corrigan, S. Measurements of the far ultraviolet reflectivity of evaporated aluminum films under exposure to O2, H2O, CO and CO2. *Vacuum* **1990**, *40*, 471–475. [CrossRef]
63. Larruquert, J.I.; Méndez, J.A.; Aznárez, J.A. Far-UV reflectance of UHV-prepared Al films and its degradation after exposure to O2. *Appl. Opt.* **1994**, *33*, 3518. [CrossRef]
64. Larruquert, J.I.; Méndez, J.; Aznárez, J. Degradation of far ultraviolet reflectance of aluminum films exposed to atomic oxygen. In-orbit coating application. *Opt. Commun.* **1996**, *124*, 208–215.
65. Larruquert, J.I.; Méndez, J.A.; Aznárez, J.A. Life prolongation of far ultraviolet reflecting aluminum coatings by periodic recoating of the oxidized surface. *Opt. Commun.* **1997**, *135*, 60–64. [CrossRef]
66. Hass, G.; Hunter, W.R. Laboratory Experiments to Study Surface Contamination and Degradation of Optical Coatings and Materials in Simulated Space Environments. *Appl. Opt.* **1970**, *9*, 2101. [CrossRef]
67. Ignatiev, A.; Chu, C.W. A proposal for epitaxial thin film growth in outer space. *Metall. Trans. A* **1988**, *19*, 2639–2643. [CrossRef]
68. Naumann, R.J. Prospects for a contamination-free ultravacuum facility in low-Earth orbit. *J. Vac. Sci. Technol. A Vac. Surf. Film.* **1989**, *7*, 90–99. [CrossRef]
69. Quijada, M.A.; Sheikh, D.A.; Del Hoyo, J.Z.G.; Richardson, J.G. ZERODUR(R) substrates for application of high-temperature protected-aluminum far-ultraviolet coatings. In *Astronomical Optics: Design, Manufacture, and Test of Space and Ground Systems II, Proceedings of the SPIE Optical Engineering + Applications, San Diego, CA, USA, 11–15 August 2019*; SPIE: Bellingham, WA, USA, 2019; p. 25.
70. Keski-Kuha, R.A.; Bowers, C.W.; Quijada, M.A.; Heaney, J.B.; Gallagher, B.; McKay, A.; Stevenson, I. James Webb Space Telescope optical telescope element mirror coatings. In *Space Telescopes and Instrumentation 2012: Optical, Infrared, and Millimeter Wave, Proceedings of the SPIE Astronomical Telescopes + Instrumentation, Amsterdam, The Netherlands, 1–6 July 2012*; Clampin, M.C., Fazio, G.G., MacEwen, H.A., Oschmann, J.M., Eds.; SPIE: Bellingham, WA, USA, 2012; p. 84422J.
71. Banyal, R.K.; Ravindra, B. Thermal characteristics of a classical solar telescope primary mirror. *N. Astron.* **2011**, *16*, 328–336. [CrossRef]
72. Li, R.; Shi, H.L.; Chen, Z.P. Study on Thermal Analysis of Main Mirror in Space Solar Telescope. *Adv. Mater. Res.* **2011**, 300–304, 328–330.
73. Onaka, T.; Kaneda, H.; Kawada, M.; Enya, K.; Nakagawa, T. Cryogenic silicon carbide mirrors for infrared astronomical telescopes: Lessons learnt from AKARI for SPICA. In *Material Technologies and Applications to Optics, Structures, Components, and Sub-Systems, Proceedings of the SPIE Optical Engineering + Applications, San Diego, CA, USA, 25–29 August 2013*; Robichaud, J.L., Krödel, M., Goodman, W.A., Eds.; SPIE: Bellingham, WA, USA, 2013; p. 88370K.
74. Middelmann, T.; Walkov, A.; Bartl, G.; Schödel, R. Thermal expansion coefficient of single-crystal silicon from 7 K to 293 K. *Phys. Rev. B* **2015**, *92*, 174113. [CrossRef]
75. Eng, R.; Arnold, W.R.; Baker, M.A.; Bevan, R.M.; Burdick, G.; Effinger, M.R.; Gaddy, D.E.; Goode, B.K.; Hanson, C.; Hogue, W.D.; et al. Cryogenic optical performance of a lightweighted mirror assembly for future space astronomical telescopes: Correlating optical test results and thermal optical model. In *Proceedings of the SPIE Optical Engineering + Applications, San Diego, CA, USA, 25–29 August 2013*; Robichaud, J.L., Krödel, M., Goodman, W.A., Eds.; SPIE: Bellingham, WA, USA, 2013; p. 88370B.
76. Poletto, L.; Naletto, G.; Tondello, G.; Patelli, A.; Rigato, V.; Salmaso, G.; Silvestrini, D.; Larruquert, J.I.; Mendez, J.A. *Grazing-Incidence Reflectivity of Si-Au Coatings for Optics with High Thermal Load*; International Society for Optics and Photonics: Bellingham, WA, USA, 2004; p. 344.
77. Gutiérrez-Luna, N.; Perea-Abarca, B.; Espinosa-Yáñez, L.; Honrado-Benítez, C.; De Lis, T.; Rodríguez-de Marcos, L.V.; Aznárez, J.A.; Larruquert, J.I. Temperature Dependence of AlF3 Protection on Far-UV Al Mirrors. *Coatings* **2019**, *9*, 428. [CrossRef]
78. Scurti, F.; Mcgarrahan, J.; Schwartzt, J. Effects of metallic coatings on the thermal sensitivity of optical fiber sensors at cryogenic temperatures. *Opt. Mat. Express* **2017**, *7*, 1754–1766. [CrossRef]
79. Wang, F.; Li, S.; Zhang, Z.; Wang, Z.; Zhou, H.; Huo, T. Effect of MgF2 deposition temperature on Al mirrors in vacuum ultraviolet. In *Proceedings of the Tenth International Conference on Thin Film Physics and Applications (TFPA 2019), Qingdao, China, 19–22 May 2019*; Chu, J., Shao, J., Eds.; SPIE: Bellingham, WA, USA, 2019; p. 42.
80. Heaney, J.B.; Kauder, L.R.; Bradley, S.E.; Neuberger, D.E. *Mirror Degradation in Orbit due to Space Radiation Exposure*; International Society for Optics and Photonics: Bellingham, WA, USA, 2000; p. 339.

81. Fuqua, P.D.; Morgan, B.A.; Adams, P.M.; Meshishnek, M.J. *Optical Darkening During Space Environmental Effects Testing-Contaminant Film Analyses*; The Aerospace Corporation: El Segundo, CA, USA, 2004.
82. Heaney, J.B.; Kauder, L.R.; Bradley, S.E.; Neuberger, D.E. Mirror degradation in orbit due to space radiation exposure. *Earth Obs. Syst. V* **2000**, *4135*, 339.
83. Dever, J.; Pietromica, A.; Stueber, T.; Sechkar, E.; Messer, R. Simulated space vacuum ultraviolet (VUV) exposure testing for polymer films. In *Proceedings of the 39th Aerospace Sciences Meeting and Exhibit; Reno, NV, USA, 8–11 January 2001*; American Institute of Aeronautics and Astronautics: Reston, VA, USA, 2001.
84. Heltzel, S.; Semprimoschnig, C.O.A.; Van Eesbeek, M.R.J. Environmental Testing of Thermal Control Materials at Elevated Temperature and Intense Ultraviolet Radiation. *J. Spacecr. Rockets* **2009**, *46*, 248–254. [CrossRef]
85. Cesul, B.T.; Mall, S.; Matson, L. Optical Response of Metakaolin after Ultraviolet and High Energy Electron Exposure. *J. Mater.* **2014**, *2014*, 1–5. [CrossRef]
86. Hass, G.; Heaney, J.B.; Hunter, W.R.; Angel, D.W. Effect of UV irradiation on evaporated ZnS films. *Appl. Opt.* **1980**, *19*, 2480. [CrossRef] [PubMed]
87. Fuqua, P.D.; Barrie, J.D.; Meshishnek, M.J.; Ciofalo, M.R.; Chu, C.T.; Chaney, J.A.; Moision, R.M. On-orbit degradation of silver mirrors exposed to ultraviolet radiation. *Opt. InfoBase Conf. Pap.* **2013**, 2011–2013.
88. Kerr, G.D.; Williams, M.W.; Birkhoff, R.D.; Painter, L.R. Optical Properties of Some Silicone Diffusion-Pump Oils in the Vacuum Ultraviolet—Using an Open-Dish Technique. *J. Appl. Phys.* **1971**, *42*, 4258–4261. [CrossRef]
89. Muscari, J.A. *Absorption Spectra of Typical Space Materials in the Vacuum Ultraviolet*; International Society for Optics and Photonics: Bellingham, WA, USA, 1981; pp. 195–200.
90. Osantowski, J.F. *Contamination Sensitivity of Typical Mirror Coatingsa Parametric Study*; International Society for Optics and Photonics: Bellingham, WA, USA, 1983; pp. 80–87.
91. Welsh, B.Y.; Jelinsky, S. *The Effect of Out-Gassing from Commonly Used Spacecraft/Space Instrument Materials on the UV-Visible-IR Reflectivity of Optical Surfaces*; International Society for Optics and Photonics: Bellingham, WA, USA, 2005; p. 58970B.
92. Meier, S.R.; Tveekrem, J.L.; Keski-Kuha, R.A.M. A far-ultraviolet contamination-irradiation facility for in situ reflectance measurements. *Rev. Sci. Instrum.* **1998**, *69*, 3642–3644. [CrossRef]
93. Canfield, L.R.; Hass, G.; Waylonis, J.E. Further Studies on MgF_2-Overcoated Aluminum Mirrors with Highest Reflectance in the Vacuum Ultraviolet. *Appl. Opt.* **1966**, *5*, 45. [CrossRef]
94. Tveekrem, J.L.; Leviton, D.B.; Fleetwood, C.M.; Feinberg, L.D. Contamination-induced degradation of optics exposed to the Hubble Space Telescope interior. *Opt. Syst. Contam. V Stray Light Syst. Optim.* **1996**, *2864*, 246–257.
95. Heaney, J.B.; Herzig, H.; Osantowski, J.F. Auger spectroscopic examination of MgF_2-coated Al mirrors before and after uv irradiation. *Appl. Opt.* **1977**, *16*, 1886. [CrossRef]
96. Quijada, M.A.; Henry, R.M.; Madison, T.; Boucarut, R.; Hagopian, J.G. *Post-Flight Reflectance of COSTAR and WF/PC 2 Pickoff Mirrors upon Their Return from Space*; International Society for Optics and Photonics: Bellingham, WA, USA, 2010; p. 77392J.
97. Osantowski, J.F.; Fleetwood, C.F. *Contamination of Grazing Incidence EUV Mirrors—An Assessment*; International Society for Optics and Photonics: Bellingham, WA, USA, 1988; p. 306.
98. Mrowka, S.; Jelinsky, S.; Jelinsky, P.; Malina, R.F. *Contamination Control Approach for The Extreme Ultraviolet Explorer Satellite Instrumentation*; International Society for Optics and Photonics: Bellingham, WA, USA, 1987; p. 34.
99. George, J.S.; Lave, K.A.; Wiedenbeck, M.E.; Binns, W.R.; Cummings, A.C.; Davis, A.J.; de Nolfo, G.A.; Hink, P.L.; Israel, M.H.; Leske, R.A.; et al. Elemental Composition And Energy Spectra Of Galactic Cosmic Rays During Solar Cycle 23. *Astrophys. J.* **2009**, *698*, 1666–1681. [CrossRef]
100. McComas, D.J.; Bame, S.J.; Barraclough, B.L.; Feldman, W.C.; Funsten, H.O.; Gosling, J.T.; Riley, P.; Skoug, R.; Balogh, A.; Forsyth, R.; et al. Ulysses' return to the slow solar wind. *Geophys. Res. Lett.* **1998**, *25*, 1–4. [CrossRef]
101. Allen, C.S.; Giraudo, M.; Moratto, C.; Yamaguchi, N. Spaceflight environment. In *Space Safety and Human Performance*; Elsevier: Amsterdam, The Netherlands, 2018; pp. 87–138.
102. Bourdarie, S.; Xapsos, M. The near-Earth space radiation environment. *IEEE Trans. Nucl. Sci.* **2008**, *55*, 1810–1832. [CrossRef]

103. Heber, B.; Potgieter, M.S.; Ferreira, S.E.S.; Dalla, S.; Kunow, H.; Müller-Mellin, R.; Wibberenz, G.; Paizis, C.; Sarri, G.; Marsden, R.G.; et al. An overview of Jovian electrons during the distant Ulysses Jupiter flyby. *Planet. Space Sci.* **2007**, *55*, 1–11. [CrossRef]
104. Naletto, G.; Boscolo, A.; Wyss, J.; Quaranta, A. Effects of proton irradiation on glass filter substrates for the Rosetta mission. *Appl. Opt.* **2003**, *42*, 3970. [CrossRef] [PubMed]
105. Pelizzo, M.G.; Corso, A.J.; Tessarolo, E.; Zuppella, P.; Böttger, R.; Huebner, R.; Della Corte, V.; Palumbo, P.; Taglioni, G.; Preti, G.; et al. *Optical Components in Harsh Space Environment*; International Society for Optics and Photonics: Bellingham, WA, USA, 2016; p. 99810G.
106. Di Sarcina, I.; Grilli, M.L.; Menchini, F.; Piegari, A.; Scaglione, S.; Sytchkova, A.; Zola, D. Behavior of optical thin-film materials and coatings under proton and gamma irradiation. *Appl. Opt.* **2014**, *53*, A314. [CrossRef]
107. Rousseau, A.D.; Windt, D.L.; Winter, B.; Harra, L.; Lamoureux, H.; Eriksson, F. *Stability of EUV Multilayers to Long-Term Heating, and to Energetic Protons and Neutrons, for Extreme Solar Missions*; International Society for Optics and Photonics: Bellingham, WA, USA, 2005; p. 590004.
108. Pelizzo, M.G.; Corso, A.J.; Tessarolo, E.; Böttger, R.; Hübner, R.; Napolitani, E.; Bazzan, M.; Rancan, M.; Armelao, L.; Jark, W.; et al. Morphological and Functional Modifications of Optical Thin Films for Space Applications Irradiated with Low-Energy Helium Ions. *ACS Appl. Mater. Interfaces* **2018**, *10*, 34781–34791. [CrossRef]
109. Pellicori, S.F.; Martinez, C.L.; Hausgen, P.; Wilt, D. Development and testing of coatings for orbital space radiation environments. *Appl. Opt.* **2014**, *53*, A339. [CrossRef] [PubMed]
110. Wei, Q.; Liu, H.; Wang, D.; Liu, S.-X. Degradation in optical reflectance of Al film mirror induced by proton irradiation. *Thin Solid Films* **2011**, *519*, 5046–5049. [CrossRef]
111. Hai, L.; Qiang, W.; Shi-Yu, H.; Dan, Z. Proton radiation effects on optical constants of Al film reflector. *Chinese Phys.* **2006**, *15*, 1086–1089. [CrossRef]
112. Qiang, W.; Hai, L.; Shi-Yu, H.; Zhen-duo, C.; Kleiman, J.I. *Characterization of Surface Morphology Changes Induced by Proton Irradiation of an Aluminum Film Reflector*; American Institute of Physics: College Park, MD, USA, 2009; pp. 657–664.
113. Qiang, W.; Dan, W.; Shengxian, L.; Hai, L. The effects of 60 keV proton irradiation on aluminum film reflector. *Spacecr. Environm. Eng.* **2010**, *27*, 434–436.
114. Gillette, R.B.; Kenyon, B.A. Proton-Induced Contaminant Film Effects on Ultraviolet Reflecting Mirrors. *Appl. Opt.* **1971**, *10*, 545. [CrossRef]
115. Zuccon, S.; Napolitani, E.; Tessarolo, E.; Zuppella, P.; Corso, A.J.; Gerlin, F.; Nardello, M.; Pelizzo, M.G. Effects of helium ion bombardment on metallic gold and iridium thin films. *Opt. Mater. Express* **2015**, *5*, 176. [CrossRef]
116. Wang, W.; Roth, J.; Lindig, S.; Wu, C. Blister formation of tungsten due to ion bombardment. *J. Nucl. Mater.* **2001**, *299*, 124–131. [CrossRef]
117. Livengood, R.; Tan, S.; Greenzweig, Y.; Notte, J.; McVey, S. Subsurface damage from helium ions as a function of dose, beam energy, and dose rate. *J. Vac. Sci. Technol. B Microelectron. Nanom. Struct.* **2009**, *27*, 3244. [CrossRef]
118. Raineri, V.; Coffa, S.; Szilágyi, E.; Gyulai, J.; Rimini, E. He-vacancy interactions in Si and their influence on bubble formation and evolution. *Phys. Rev. B* **2000**, *61*, 937–945. [CrossRef]
119. Pelizzo, M.G.; Corso, A.J.; Zuppella, P.; Windt, D.L.; Mattei, G.; Nicolosi, P. Stability of extreme ultraviolet multilayer coatings to low energy proton bombardment. *Opt. Express* **2011**, *19*, 14838. [CrossRef]
120. Nardello, M.; Zuppella, P.; Polito, V.; Corso, A.J.; Zuccon, S.; Pelizzo, M.G. Stability of EUV multilayer coatings to low energy alpha particles bombardment. *Opt. Express* **2013**, *21*, 28334. [CrossRef]
121. Delmotte, F.; Meltchakov, E.; de Rossi, S.; Bridou, F.; Jérome, A.; Varnière, F.; Mercier, R.; Auchère, F.; Zhang, X.; Borgo, B.; et al. *Development of Multilayer Coatings for Solar Orbiter EUV Imaging Telescopes*; International Society for Optics and Photonics: Bellingham, WA, USA, 2013; p. 88620A.
122. Kuznetsov, A.S.; Gleeson, M.A.; Bijkerk, F. Ion effects in hydrogen-induced blistering of Mo/Si multilayers. *J. Appl. Phys.* **2013**, *114*, 113507. [CrossRef]
123. Kuznetsov, A.S.; Gleeson, M.A.; Bijkerk, F. Hydrogen-induced blistering of Mo/Si multilayers: Uptake and distribution. *Thin Solid Films* **2013**, *545*, 571–579. [CrossRef]

124. Van de Ven, T.H.M.; Reefman, P.; De Meijere, C.A.; Van der Horst, R.M.; van Kampen, M.; Banine, V.Y.; Beckers, J. Ion energy distributions in highly transient EUV induced plasma in hydrogen. *J. Appl. Phys.* **2018**, *123*, 063301. [CrossRef]
125. Douglas Caswell, R.; McBride, N.; Taylor, A. Olympus end of life anomaly—A perseid meteoroid impact event? *Int. J. Impact Eng.* **1995**, *17*, 139–150. [CrossRef]
126. *Limiting Future Collision Risk to Spacecraft: An Assessment of NASA's Meteoroid and Orbital Debris Programs*; National Academies Press: Washington, DC, USA, 2011; ISBN 978-0-309-21974-7.
127. Jones, J. *Meteoroid Engineering Model—Final Report*; National Aeronautics and Space Administration: Washington, DC, USA, 2004.
128. Drolshagen, G.; Carey, W.; McDonnell, J.A.; Stevenson, T.; Mandeville, J.; Berthoud, L. HST solar array impact survey: Revised damage laws and residue analysis. *Adv. Sp. Res.* **1997**, *19*, 239–251. [CrossRef]
129. Young, R.P. Low-Scatter Mirror Degradation by Particle Contamination. *Opt. Eng.* **1976**, *15*, 156516. [CrossRef]
130. Stübig, M.; Schäfer, G.; Ho, T.-M.; Srama, R.; GrunGrün, E. Laboratory simulation improvements for hypervelocity micrometeorite impacts with a new dust particle source. *Planet. Space Sci.* **2001**, *49*, 853–858. [CrossRef]
131. Heaney, J.B.; Pearl, J.C.; Stuebig, M.A.; Wang, L.L.; He, C.C. Hypervelocity particle impact studies performed on a gold-coated beryllium substrate mirror. *Opt. Infrared Millim. Sp. Telesc.* **2004**, *5487*, 1100.
132. Graham, G.A.; Kearsley, A.T.; Drolshagen, G.; McBride, N.; Green, S.F.; Wright, I.P. Microparticle impacts upon HST solar cells. *Adv. Sp. Res.* **2001**, *28*, 1341–1346. [CrossRef]
133. See, T.; Allbrooks, M.; Atkinson, D.; Simon, C.Z.M. *Meteoroid and Debris Impact Features Documented on The Long Duration Exposure Facility: A Preliminary Report*; National Aeronautics and Space Administration: Washington, DC, USA, 1990.
134. Hawkins, G.J.; Hunneman, R.; Seeley, J.S. *Space Exposure of Infrared Filters and Materials on the NASA Long Duration Exposure Facility (LDEF)*; Space Expo: Noordwijk, The Netherlands, 1991.
135. Whipple, F.L. Meteorites and space travel. *Astron. J.* **1947**, *52*, 131. [CrossRef]